Energy loss of swift projectiles with n ($n \leq 4$) bound electrons

Toshiaki Kaneko
Department of Applied Physics, Okayama University of Science, Ridaicho, Okayama 700, Japan
(Received 8 December 1992)

Based on first-order perturbation theory and the frozen-charge-state model, an analytical formula for the electronic stopping power was derived for swift lithiumlike and berylliumlike ions. The bound electrons attached to ions in the ground state were described by the Hartree-Fock-Slater determinant, in which the orbital-screening parameter in the constituent eigenfunctions was determined by the variational method. The stopping power $-dE/dx$ for fast hydrogenlike to berylliumlike ions is found to be scaled in terms of $(-dE/dx)Z_1^{-\alpha}$ where α ranges from 2.180 (H-like) to 2.355 (Be-like). The theoretical stopping for Li-like ions agrees quite well with the recent data on ~ 10 MeV/amu O^{5+} ions.

PACS number(s): 34.50.Bw, 61.80.Mk

I. INTRODUCTION

In the penetration of swift charged particles through matter, inelastic energy losses have been fundamental and essential problems in the fields of atomic collisions in solids and plasma–first-wall interactions. This is because this quantity is directly related to energy deposition in a material by impinging ions, to the range which they can attain on average, and to the emission yields of secondary electrons, ions, and atoms.

The electronic stopping power of materials for fast ionized projectiles has been investigated intensively. From the experimental viewpoint, many measurements have provided stopping-power data for gases and solid media [1,2]. Theoretical procedures, on the other hand, have been based on the atomic model [3,4], the free-electron-gas model [5–7], the kinetic model [8], a nonlinear calculation [9], the local-density model [10,11], and the wave-packet model [12]. Recently, theoretical data tables for the stopping power for a proton have also been presented [13,14].

Early theoretical works were initiated by Bethe and Bloch within the point-charge picture [3,4]. For a swift point charge $Z_1 e$ moving at velocity v in a material with atomic number Z_2, the inelastic energy loss per unit of the primary path is given [3] by

$$S=(4\pi e^4/mv^2)NZ_2Z_1^2\ln(2mv^2/I)\ . \tag{1.1}$$

In the above, m and e are the electron rest mass and the elementary charge. N and I denote, respectively, the number density and the mean excitation energy of the target atoms. Later, this Bethe formula was extended to include the higher-order terms, i.e., the Barkas term (or Z_1^3 term) [15] and the Bloch term (Z_1^4 term) [4], together with the shell correction [16], resulting in a standard formula for the energy loss of fully stripped swift light ions.

The energy loss of partially stripped ions (PSI's) was, for the first time, treated by Ferrell and Ritchie [17] for a slow He^+ ion moving in a degenerate electron gas. When the number of bound electrons on a projectile is large enough, a PSI may be well described by a Thomas-Fermi statistical model and its energy loss in the electron gas can be formulated [18,19] in a way similar to the treatment of Ferrell and Ritchie. For PSI's we are concerned with the question to what extent the bound electrons diminish the energy loss of the projectile. In order to answer this, the concept of the effective charge $Z_{\rm eff}$ is very useful [20]; it is defined as the square root of the stopping power for a projectile relative to that for a proton moving in the same material at the same velocity. In general there are two quantities of a projectile, i.e., the spatial size and the average number of bound electrons, contributing to the effective charge.

In recent experiments, it has become possible to measure directly the energy loss of frozen-charge-state PSI's [21–23]. In particular, with the use of a very-high-resolution analyzer, Ogawa *et al.* [22,23] directly measured the energy loss of fast hydrogenlike (He^+, O^{7+}, C^{5+}) and heliumlike (O^{6+},C^{4+}) ions passing through thin carbon foils with kinetic energy 10.6 MeV/amu and with charge equal to the incident-ion charge. An analytical stopping-power formula for those fast ions was derived in the following form [24]:

$$S=(4\pi e^4/mv^2)NZ_2L(Z_1,Z_2,v)\ , \tag{1.2a}$$

$$\begin{aligned} L(Z_1,Z_2,v)=&(Z_1-N_{1s})^2\ln(2mv^2/I)\\ &+(2Z_1N_{1s}-N_{1s}^2)\ln\{v/(Z_e v_0)\}\\ &+Z_1N_{1s}-(\tfrac{11}{12})N_{1s}^2\ . \end{aligned} \tag{1.2b}$$

Here the Barkas term, the Bloch term, and the shell correction are neglected. In Eq. (1.2b), N_{1s} denotes the number of $1s$ electrons, so that we set $Z_e=Z_1$ and $N_{1s}=1$ for hydrogenlike projectiles, and $Z_e=Z_1-\frac{5}{16}$ and $N_{1s}=2$ for heliumlike ones. The quantity Z_e is related to the orbital screening parameter which will appear in the next section. Quite recently, Ogawa *et al.* [25] also reported the stopping power of carbon for the 169-MeV lithiumlike O^{5+} ion for the first time.

In this paper we present analytical formulas for the electronic energy loss of swift lithiumlike and berylliumlike ions within the framework of the Born approximation. We assume that the charge state of the projectile

remains frozen during its passage. Section II is devoted to a description of the present approach. First, the spatial distribution of the bound electrons on a projectile is determined by minimizing the total energy, using a variational method. Secondly, analytical results for the stopping power are derived and the degree of screening per bound electron is discussed. Finally, comparison of the theoretical results is made with recent experimental data. Throughout this paper, m, e, a_0, v_0, and $\hbar$ denote the electron rest mass, the elementary charge, the Bohr radius (0.529×10^{-8} cm), the Bohr velocity (2.19×10^{8} cm/s), and the Planck constant divided by 2π, respectively.

II. THEORY

Here we consider the case where the velocity v of a projectile is higher than both the statistical average velocity $Z_2^{2/3}v_0$ of the target electrons and the velocity $Z_e v_0$ of the bound electrons on the projectile. Our procedure is based on first-order perturbation treatment, so that the formulas derived later for swift PSI's correspond to the Bethe expression (1.1) in the sense of having the same theoretical base. Other correction terms are all neglected.

First of all, we discuss the validity of the present theory, developed under the pre-equilibrium charge-state condition. In the velocity range of $v > Z_e v_0$, the electron loss process is much more dominant than the electron capture process, as the velocity-stripping criterion suggests [26]. In a very thin region, the charge fraction ϕ_i of particles penetrating to depth d with charge i equal to the incident charge decreases as $\exp(-d/\lambda_i)$. With increasing d, due to electron capture, ϕ_i deviates from a simple exponential function. After enough penetration, it finally reaches the equilibrium fraction $\phi_i^{\rm eq}$, depending on velocity but no longer on d. The attenuation length λ_i is given by the sum of charge-changing cross sections $\sigma_{i,j}$ from charge state i to j ($\neq i$), such that $\lambda_i = 1/(\sum_{j(\neq i)} N\sigma_{i,j})$. N is the number of target atoms per unit volume. At high velocities, $\phi_i^{\rm eq}$ is very small (e.g., 10^{-5} for a 10-MeV/amu He^+ ion [22]) and λ_i is approximately given by $1/(\sigma_{\rm loss}N)$, where $\sigma_{\rm loss}$ ($=\sigma_{i,i+1}$) is the one-electron-loss cross section. Therefore, the pre-equilibrium charge-state depth $d_{\rm pre}$ is approximately characterized by

$$d_{\rm pre} = \ln(1/\phi_{\rm eq})/(\sigma_{\rm loss}N) \ . \tag{2.1}$$

As an example, the value of $d_{\rm pre}$ for 10.6-MeV/amu C^{q+} ($q=4,5$) ions penetrating a carbon foil is at least more than 50 μg/cm^2 [25]. In order to compare with the present theory, measurements should be performed using foils of thickness less than $d_{\rm pre}$.

A. Description of bound electrons

Here we focus on the electron distribution $\rho(\mathbf{r})$ in a ground-state projectile under the frozen charge state. For convenience, we consider a berylliumlike projectile having 4 electrons in the $1s^2 2s^2$ singlet configuration. As we shall see later, a lithiumlike projectile can be treated in a similar manner. It is very reasonable to assume that $\rho(\mathbf{r})$ is spherically symmetric unless any directional electric field is acting on the projectile. Then only the s-type wave functions are considered. They consist of hydrogenic $1s$ and $2s$ wave functions including an adequate screening parameter. In order to determine this reasonably, the total energy of the system is first calculated in a quantum-mechanical manner. The Hamiltonian of our system is written as

$$H = \sum_i H_i + \tfrac{1}{2}\sum_{\substack{i,j \\ i\neq j}} V_{ij} \ , \tag{2.2a}$$

$$H_i = (-\hbar^2/2m)\Delta_i - Z_1 e^2/r_i \ , \tag{2.2b}$$

$$V_{ij} = e^2/|\mathbf{r}_i - \mathbf{r}_j| \ . \tag{2.2c}$$

The wave function Ψ is described by a Hartree-Fock-Slater determinant:

$$\Psi = (4!)^{-1/2}\begin{vmatrix} \psi_{1s}(\mathbf{r}_1)\alpha & \psi_{1s}(\mathbf{r}_1)\beta & \psi_{2s}(\mathbf{r}_1)\alpha & \psi_{2s}(\mathbf{r}_1)\beta \\ \psi_{1s}(\mathbf{r}_2)\alpha & \psi_{1s}(\mathbf{r}_2)\beta & \psi_{2s}(\mathbf{r}_2)\alpha & \psi_{2s}(\mathbf{r}_2)\beta \\ \psi_{1s}(\mathbf{r}_3)\alpha & \psi_{1s}(\mathbf{r}_3)\beta & \psi_{2s}(\mathbf{r}_3)\alpha & \psi_{2s}(\mathbf{r}_3)\beta \\ \psi_{1s}(\mathbf{r}_4)\alpha & \psi_{1s}(\mathbf{r}_4)\beta & \psi_{2s}(\mathbf{r}_4)\alpha & \psi_{2s}(\mathbf{r}_4)\beta \end{vmatrix} \tag{2.3a}$$

where

$$\psi_{1s}(\mathbf{r}) = (\pi a_0^3/Z_e^3)^{-1/2}\exp(-Z_e r/a_0) \ , \tag{2.3b}$$

$$\psi_{2s}(\mathbf{r}) = (4\pi)^{-1/2}(2a_0/Z_e)^{-3/2} \times (2 - Z_e r/a_0)\exp(-Z_e r/2a_0) \ , \tag{2.3c}$$

and the spin wave functions for the up-spin and down-spin state are denoted respectively by α and β. The normalized wave functions $\psi_{1s}(\mathbf{r})$ and $\psi_{2s}(\mathbf{r})$ are proved to be orthogonal to each other [27]. The constant Z_e in (2.3b) and (2.3c) denotes the orbital-screening parameter, which depends both on the number of bound electrons and on the atomic number Z_1 of a projectile. Using Eqs. (2.3a)–(2.3c), the expectation value $\langle H \rangle$ of H is calculated as

$$\langle H \rangle = 2E_{1s} + 2E_{2s} + V_{1s-1s} + 4V_{1s-2s} + V_{2s-2s} - 2A_{1s-2s} \ , \tag{2.4a}$$

where

$$E_{1s} = \hbar^2 Z_e^2/(2ma_0^2) - Z_1 e^2 Z_e/a_0 \ , \tag{2.4b}$$

$$E_{2s} = (\tfrac{1}{4})E_{1s} \ , \tag{2.4c}$$

$$V_{1s-1s} = e^2\int d\mathbf{r}\int d\mathbf{r}'|\psi_{1s}(\mathbf{r})|^2|\psi_{1s}(\mathbf{r}')|^2/|\mathbf{r}-\mathbf{r}'| = 5e^2 Z_e/(8a_0) \ , \tag{2.4d}$$

$$V_{1s-2s} = e^2\int d\mathbf{r}\int d\mathbf{r}'|\psi_{2s}(\mathbf{r})|^2|\psi_{1s}(\mathbf{r}')|^2/|\mathbf{r}-\mathbf{r}'| = 17e^2 Z_e/(81a_0) \ , \tag{2.4e}$$

$$V_{2s-2s} = e^2\int d\mathbf{r}\int d\mathbf{r}'|\psi_{2s}(\mathbf{r})|^2|\psi_{2s}(\mathbf{r}')|^2/|\mathbf{r}-\mathbf{r}'| = 77e^2 Z_e/(512a_0) \ , \tag{2.4f}$$

$$A_{1s-2s}=\int d\mathbf{r}\int d\mathbf{r}'\psi_{1s}(\mathbf{r})^*\psi_{2s}(\mathbf{r}')^*(e^2/|\mathbf{r}-\mathbf{r}'|)\times\psi_{1s}(\mathbf{r}')\psi_{2s}(\mathbf{r})=16e^2Z_e/(729a_0)\ . \tag{2.4g}$$

In the above equations, V_{1s-1s}, V_{1s-2s}, and V_{2s-2s} are the direct Coulomb integrals and A_{1s-2s} the exchange integral between electrons with parallel spin. After simple algebra, the total energy for the berylliumlike ($1s^22s^2$) system is represented as

$$\langle H\rangle_{\mathrm{Be}}=(\tfrac{5}{4})(Z_e^2-2Z_eZ_1)+(586\,373/373\,248)Z_e \tag{2.5}$$

in units of e^2/a_0. This energy takes the minimum value

$$\langle H\rangle_{\mathrm{Be}}=-(\tfrac{5}{4})Z_{\mathrm{Be}}^2(e^2/a_0) \tag{2.6}$$

at $Z_e=Z_{\mathrm{Be}}$, where

$$Z_{\mathrm{Be}}=Z_1-586\,373/933\,120=Z_1-0.6284\ . \tag{2.7}$$

In the same manner, we can obtain the expression for the total energy $\langle H\rangle_{\mathrm{Li}}$ for the lithiumlike ($1s^22s$) electron system as follows:

$$\langle H\rangle_{\mathrm{Li}}=2E_{1s}+E_{2s}+V_{1s-1s}+2V_{1s-2s}-A_{1s-2s}=(\tfrac{9}{8})(Z_e^2-2Z_eZ_1)+(5965/5832)Z_e\ , \tag{2.8}$$

in units of e^2/a_0. The minimum value of (2.8) can easily be found to be

$$\langle H\rangle_{\mathrm{Li}}=-(\tfrac{9}{8})Z_{\mathrm{Li}}^2(e^2/a_0) \tag{2.9}$$

at $Z_e=Z_{\mathrm{Li}}$, where

$$Z_{\mathrm{Li}}=Z_1-5965/13\,122=Z_1-0.454\,58\ . \tag{2.10}$$

Thus the spatial distribution of bound electrons is completely determined by the variational method. Let us invoke the total energy of the heliumlike ($1s^2$) electron system in the following:

$$\langle H\rangle_{\mathrm{He}}=2E_{1s}+V_{1s-1s}=Z_e^2-2Z_1Z_e+(\tfrac{5}{8})Z_e=(Z_e-Z_{\mathrm{He}})^2-Z_{\mathrm{He}}^2\ . \tag{2.11}$$

with

$$Z_{\mathrm{He}}=Z_1-\tfrac{5}{16}\ . \tag{2.12}$$

Because there is no pair of electrons with parallel spin, the exchange term should not appear. Thus $\langle H\rangle_{\mathrm{He}}$ takes the minimum value $(Z_1-\frac{5}{16})^2(e^2/a_0)$ at $Z_e=Z_{\mathrm{He}}$. It is interesting to compare Z_{Li} and Z_{Be} with Z_{He}. From (2.7), (2.10), and (2.12), one sees that $Z_{\mathrm{Be}}<Z_{\mathrm{Li}}<Z_{\mathrm{He}}$ for the same Z_1 value, namely, the greater the number of bound electrons, the less the orbital-screening parameter.

B. Stopping-power formula

This section is devoted to derivation of the analytical formulas for the electronic stopping power of a target material. As explained in the introduction, we treat the berylliumlike and lithiumlike projectiles in such a manner that the charge state of bound electrons is fixed and not subjected to excitation inside the target material. A general expression for the electronic stopping power in this case is given in the Born approximation as follows [28,29]:

$$S=N\sum_n(E_n-E_0)\int_{q_{\min}}^{q_{\max}}(dq/q^3)8\pi(e^2/\hbar v)^2\times|F_{00}^p(-\mathbf{q})|^2|F_{n0}^t(\mathbf{q})|^2\ . \tag{2.13}$$

In the above, E_n and E_0 denote the eigenenergies of the target states n and 0, respectively. N is the number of target atoms per unit volume. The momentum $\hbar q$ transferred to the target electrons ranges from $\hbar q_{\min}=(E_n-E_0)/v$ to $\hbar q_{\max}=2mv$. The form factor of the projectile, $F_{00}^p(-\mathbf{q})$, and the inelastic scattering amplitude of the target atom, $F_{n0}^t(\mathbf{q})$, are written as

$$F_{00}^p(-\mathbf{q})=Z_1-\left\langle\Psi\left|\sum_i\exp(+i\mathbf{q}\cdot\mathbf{r}_i)\right|\Psi\right\rangle\ , \tag{2.14}$$

$$F_{n0}^t(q)=\left\langle n\left|\sum_j\exp(-i\mathbf{q}\cdot\mathbf{r}_j)\right|0\right\rangle\ . \tag{2.15}$$

The term $\langle\Psi|\sum_i\exp(+i\mathbf{q}\cdot\mathbf{r}_i)|\Psi\rangle$ on the left-hand side of Eq. (2.14) [hereafter denoted by $\rho(\mathbf{q})$] denotes the Fourier transform of the spatial electron distribution $\rho(\mathbf{r})=\langle\Psi|\sum_i\delta(\mathbf{r}-\mathbf{r}_i)|\Psi\rangle$. We have for lithiumlike and berylliumlike projectiles

$$\rho(\mathbf{q})=2\rho_{1s}(\mathbf{q})+N_{2s}\rho_{2s}(\mathbf{q})\ , \tag{2.16a}$$

$$\rho_{1s}(\mathbf{q})=[1+(qa_0/2Z_e)^2]^{-2}\ , \tag{2.16b}$$

$$\rho_{2s}(\mathbf{q})=\frac{[2(qa_0/Z_e)^2-1][(qa_0/Z_e)^2-1]}{[1+(qa_0/Z_e)^2]^4}\ . \tag{2.16c}$$

Here N_{2s} is the number of $2s$ electrons on the projectile. Then we take $Z_e=Z_{\mathrm{Li}}$ and $N_{2s}=1$ for lithiumlike projectiles, and $Z_e=Z_{\mathrm{Be}}$ and $N_{2s}=2$ for berylliumlike ones.

It is convenient to divide the integration region $[q_{\min},q_{\max}]$ into two sections, i.e., $A=[q_{\min},q_0]$ and $B=[q_0,q_{\max}]$, where q_0 is an appropriate parameter such that the dipole approximation can be applied to $F_{n0}^t(\mathbf{q})$. Physically speaking, this means the separation of close and distant collisions. Hereby we have $\exp(-i\mathbf{q}\cdot\mathbf{r}_j)=1-i\mathbf{q}\cdot\mathbf{r}_j$ and the contribution of the distant collision (section A), S_A, is then reduced to

$$S_A=N\sum_n(E_n-E_0)8\pi(e^2/\hbar v)^2|\mathbf{d}_{n0}|^2\times\int_{q_{\min}}^{q_0}(dq/q)|F_{00}^p(-\mathbf{q})|^2\ , \tag{2.17}$$

where $\mathbf{d}_{n0}$ is the dipole-transition matrix element. On the other hand, the contribution of the close collision (section B), S_B, is expressed as

$$S_B=N(\hbar^2/2m)Z_2 8\pi(e^2/\hbar v)^2\times\int_{q_0}^{q_{\max}}(dq/q)|F_{00}^p(-\mathbf{q})|^2\ . \tag{2.18}$$

Here one can interchange the order of the summation over n and the integration over q since both $q_{\max}$ and q_0 are independent of the eigenstate $|n\rangle$. Thus we are able to employ the sum rule [27,30]

$$\sum_n (E_n - E_0)|F^t_{n0}(\mathbf{q})|^2 = (\hbar^2 q^2/2m)Z_2 \ . \tag{2.19}$$

Fortunately, the definite integrals in S_A and S_B are straightforwardly estimated if one used the following result:

$$2\int (dq/q)|F^p_{00}(-\mathbf{q})|^2 = 2A\ln(qa_0/Z_e) + f((qa_0/Z_e)^2+1) + g((qa_0/Z_e)^2+4) + \text{integral constant} \ , \tag{2.20}$$

where $f(x)$ and $g(x)$ are given by

$$f(x) = B_0\ln(x) + \sum_{j=1}^{7} B_j/x^j \ , \tag{2.21}$$

$$g(x) = C_0\ln(x) + \sum_{j=1}^{3} C_j/x^j \ . \tag{2.22}$$

In Eqs. (2.20)–(2.22), A, B_i $(i=1-7)$, and C_i $(i=1-3)$ are the following constants:

$$\begin{aligned}
A &= (Z_1 - N_{2s} - 2)^2 \ , \\
B_0 &= 2Z_1N_{2s} + (512/81)N_{2s} - N_{2s}^2 \ , \\
B_1 &= -2Z_1N_{2s} + (704/27)N_{2s} + N_{2s}^2 \ , \\
B_2 &= Z_1N_{2s} - (160/9)N_{2s} + (1/2)N_{2s}^2 \ , \\
B_3 &= -4Z_1N_{2s} + (128/9)N_{2s} + (1/3)N_{2s}^2 \ , \\
B_4 &= -(3/4)N_{2s}^2 \ , \\
B_5 &= 5N_{2s}^2 \ , \quad B_6 = -8N_{2s}^2 \ , \quad B_7 = (36/7)N_{2s}^2 \ , \\
C_0 &= 4\{Z_1 - 1 - (209/81)N_{2s}\} \ , \\
C_1 &= -16(Z_1 - 1) + (80/9)N_{2s} \ , \\
C_2 &= 32 \ , \quad C_3 = 256/3 \ .
\end{aligned} \tag{2.23}$$

We note that the factor A is the square of the net charge of the projectile. At this point, we remember that the high- (but nonrelativistic) velocity case is now considered. Then, it is reasonable to assume that the conditions $(a_0/Z_e)^2 q^2_{\min} \ll 1$, i.e., $E_n - E_0 \ll Z_{\mathrm{Li}}\hbar v/a_0$ (or $Z_{\mathrm{Be}}\hbar v/a_0$) and $(a_0/Z_e)^2 q^2_{\max} \gg 4$, i.e., $v \gg Z_{\mathrm{Li}} v_0$ (or $Z_{\mathrm{Be}} v_0$) are valid in the energy region considered. Therefore, using the sum rule [27,30],

$$\sum_n (E_n - E_0)|\mathbf{d}_{n0}|^2 = (\hbar^2/2m)Z_2 \ , \tag{2.24}$$

and the approximations $[y = (a_0 q_{\min}/Z_e)^2]$

$$f(y+1) = \sum_{i=1}^{7} B_i + \left\{ B_0 - \sum_{i=1}^{7} iB_i \right\} y + O(y^2) \ , \tag{2.25}$$

$$g(y+4) = C_0\ln 4 + \sum_{i=1}^{3} C_i/4^i + \left\{ C_0/4 - \sum_{i=1}^{3} iC_i/4^{i+1} \right\} y + O(y^2) \ , \tag{2.26}$$

we get

$$\begin{aligned}
S_A = (2\pi e^4/mv^2)NZ_2 \Big[& 2A\ln(q_0a_0/Z_e) + f((q_0a_0/Z_e)^2+1) + g((q_0a_0/Z_e)^2+4) \\
& - 2A\ln(Ia_0/Z_e\hbar v) - \sum_{i=1}^{7} B_i - C_0\ln 4 - \sum_{i=1}^{3} C_i/4^i \\
& - \left\{ B_0 - \sum_{i=1}^{7} iB_i + C_0/4 - \sum_{i=1}^{3} iC_i/4^{i+1} \right\} (2m/\hbar^2 Z_2) G_3 (a_0/\hbar v Z_e)^2 - O(G_5(a_0/\hbar v Z_e)^4) \Big] \ .
\end{aligned} \tag{2.27}$$

Here I denotes the mean excitation energy of the target, defined by

$$\ln I = (1/Z_2)(2m/\hbar^2) \sum_n (E_n - E_0)|\mathbf{d}_{n0}|^2 \ln(E_n - E_0) \ , \tag{2.28}$$

and G_m denotes the mth excitation-energy moment of the dipole transition probability, such that

$$G_m = \sum_n (E_n - E_0)^m |\mathbf{d}_{n0}|^2 \quad (m = 3, 5) \ . \tag{2.29}$$

It is easily seen that the first moment G_1 leads to the well-known sum rule (2.24).

Next let us estimate S_B. If we use the following approximations $[y = (a_0 q_{\max}/Z_e)^2]$:

$$f(y+1) = B_0\ln(y) + (B_0 + B_1)(1/y) + O(y^{-2}) \ , \tag{2.30}$$

and

$$g(y+4) = C_0\ln(y) + (4C_0 + C_1)(1/y) + O(y^{-2}) \ , \tag{2.31}$$

we finally have

$$\begin{aligned}
S_B = (2\pi e^4/mv^2)NZ_2 \big[& 2(A + B_0 + C_0)\ln(2mva_0/\hbar Z_e) - 2A\ln(q_0a_0/Z_e) - f((q_0a_0/Z_e)^2+1) \\
& - g((q_0a_0/Z_e)^2+4) + (B_0 + B_1 + 4C_0 + C_1)(\tfrac{1}{2})(\hbar Z_e/mva_0)^2 + O((2mva_0/\hbar Z_e)^{-4}) \big] \ .
\end{aligned} \tag{2.32}$$

As we evaluated separately the contributions of distant and close collisions, the sum of S_A and S_B yields the total electronic stopping power

$$S=(4\pi e^4/mv^2)NZ_2L(Z_1,Z_2,v)\ , \tag{2.33a}$$

with

$$L(Z_1,Z_2,v)=(Z_1-N_{2s}-2)^2\ln(2mv^2/I)+\{2Z_1N_{2s}+(512/81)N_{2s}-N_{2s}^2\}\ln(2v/Z_ev_0)$$
$$+4\{Z_1-1-(209/81)N_{2s}\}\ln(v/Z_ev_0)+2Z_1+(5/2)Z_1N_{2s}-(334/27)N_{2s}-11/3-(271/168)N_{2s}^2\ , \tag{2.33b}$$

where $Z_e=Z_{\rm Li}$ and $N_{2s}=1$ for lithiumlike projectiles, and $Z_e=Z_{\rm Be}$ and $N_{2s}=2$ for berylliumlike ones. Here we note that the terms of the order of v^{-2} and those of the order of v^{-4} in the square brackets in Eqs. (2.27) and (2.32) are both dropped in Eq. (2.33). The former plays the role of the leading correction to $L(Z_1,Z_2,v)$ as follows:

$$\Delta L=-\left[(7/4)(Z_1-N_{2s})N_{2s}-(133/27)N_{2s}+Z_1-2\right]$$
$$\times(2mG_3/\hbar^2Z_2)/(mv_0vZ_e)^2\ . \tag{2.34}$$

Let us return to the leading expression (2.33). We remark here that the target is characterized by three quantities (I, Z_2, and N), and that the separation parameter q_0 cancels out in the final expression (2.33). It is of interest that the first term of (2.33b) is interpreted as Bethe's original form for a net charge $(Z_1-N_{2s}-2)$. This comes from the logarithmic term in (2.20). There the spatial size of the projectile is completely neglected. The other terms might be regarded as correction terms to such a crude description. However this is not correct, since these terms actually contribute comparably with the first term. This fact will be seen in the next section on the effective charge.

As an application of Eq. (2.33), a brief comment is given on the stopping power for swift neutral-atom projectiles. The quantity L of Eq. (2.33b) for hydrogen, helium, lithium, and beryllium atom respectively reduces to

$$L_{\rm H}=\ln(v/v_0)+\tfrac{1}{12}\ , \tag{2.35a}$$

$$L_{\rm He}=4\ln(16v/27v_0)+\tfrac{1}{3}\ , \tag{2.35b}$$

$$L_{\rm Li}=9\ln(13\,122v/33\,401v_0)$$
$$+(917/81)\ln2-6275/1512\ , \tag{2.35c}$$

$$L_{\rm Be}=16\ln(933\,120v/3\,146\,107v_0)$$
$$+(1996/81)\ln2-2593/378\ . \tag{2.35d}$$

We remark that the above expressions do not contain the characteristic parameter I, and depend only on the macroscopic parameters N and Z_2, as for a target. Hence the stopping cross section for these atoms *in the charge-state pre-equilibrium region* is merely proportional to the target atomic number Z_2. To see the cancellation of I in detail, let us get back to Eq. (2.20). One realizes that the logarithmic term $\ln(I)$ originates from the integration of $1/q$ over q. In other words, a pure Coulomb interaction between collision partners plays an essential role. In the cases of neutral-atom projectiles, the net charge vanishes so that the interaction becomes short range rather than a pure Coulomb interaction. Consequently, the term $\ln(I)$ vanishes in (2.35).

C. Effective charge and the degree of screening by projectile electrons

In this section we discuss the effective charge $Z_{\rm eff}$ of the projectile and estimate the screening charge per bound electron by subtracting the $Z_{\rm eff}$ value for an ion in charge state q from the $Z_{\rm eff}$ in charge state $q-1$. In order to comprehend and compile the stopping-power data, the concept of the effective charge is useful. This idea is based on the proportionality of the Bethe formula to the square of the incident charge. The effective charge is defined as the square root of the ratio of the stopping power S to the proton stopping power S_p at the same velocity:

$$Z_{\rm eff}=(S/S_p)^{1/2}\ . \tag{2.36}$$

The idea of the effective charge is to condense various effects on the electronic excitation, e.g., the spatial size and charge-changing effects, into only one parameter $Z_{\rm eff}$. Using the definition of $Z_{\rm eff}$, the quantity $L(Z_1,Z_2,v)$ of Eq. (2.33b) is written as $(Z_{\rm eff})^2\ln(2mv^2/I)$.

In general, the effective charge has two aspects. One is the charge-exchange effect and the other is the spatial size effect. The former is represented by stripping bound electrons more and more to become a bare nucleus with increasing velocity. On the other hand, the spatial size effect enlarges the contribution of close collisions, where the target electrons are scattered by a projectile with effective charge greater than its net charge. This is due to incomplete screening of the nuclear charge by bound electrons. In the case of frozen-charge-state ions, the electron distribution is assumed to be fixed during passage even at high velocities. In this sense, the effective charge of frozen-charge-state ions contains only the size effect.

Let us find an explicit representation for $Z_{\rm eff}$ of ions in a frozen charge state. From Eq. (2.33b) and the definition of $Z_{\rm eff}$, we easily find

$$Z_{\text{eff}}^2=(Z_1-N_{2s}-2)^2+[\ln(2mv^2/I)]^{-1}[\{2Z_1N_{2s}+(512/81)N_{2s}-N_{2s}^2\}\ln(2v/Z_ev_0)$$
$$+4\{Z_1-1-(209/81)N_{2s}\}\ln(v/Z_ev_0)+2Z_1+(5/2)Z_1N_{2s}$$
$$-(334/27)N_{2s}-11/3-(271/168)N_{2s}^2]\ . \tag{2.37}$$

In the high-velocity limit, i.e., when $v\gg Z_ev_0$ and $v\gg(I/2m)^{1/2}$, Z_{eff} in Eq. (2.37) approaches the asymptotic value

$$Z_{\text{eff}}^2=\tfrac{1}{2}\{(Z_1-N_{2s}-2)^2+Z_1^2\}\ , \tag{2.38}$$

which is independent of velocity.

In order to compare with other cases, we write the expression for Z_{eff} for hydrogenlike and heliumlike projectiles:

$$Z_{\text{eff}}^2=(Z_1-N_{1s})^2+[\ln(2mv^2/I)]^{-1}[(2Z_1N_{1s}-N_{1s}^2)\ln(v/Z_ev_0)+Z_1N_{1s}-(12/11)N_{1s}^2]\ . \tag{2.39}$$

At high velocities, Eq. (2.39) also reduces to the velocity-independent value

$$Z_{\text{eff}}^2=\tfrac{1}{2}\{(Z_1-N_{1s})^2+Z_1^2\}\ . \tag{2.40}$$

Equations (2.38) and (2.40) mean that in the high-velocity limit the square of the effective charge is the arithmetic average of the square of the nuclear charge of a projectile and the square of the net charge [31]. This relation means there are equal contributions from two extreme cases, i.e., complete neglect of bound electrons and complete screening of the nucleus.

Once the effective charge $Z_{\text{eff}}(q)$ of an ion in charge state q $(=Z_1-N_{1s}-N_{2s})$ is obtained from Eq. (2.37) or (2.39), we can estimate the magnitude of screening by a bound electron. Here we define the screening charge $Z_{\text{SC}}(q,q-1)$ by

$$Z_{\text{SC}}(q,q-1)=Z_{\text{eff}}(q)-Z_{\text{eff}}(q-1)\ . \tag{2.41}$$

Later, we concentrate on screening by $1s$ and $2s$ electrons. This quantity will be found to show the shell effect.

III. NUMERICAL RESULTS, COMPARISON, AND DISCUSSION

First we discuss the validity of the choice of wave function. It is rather reasonable [32] to describe the ground-state berylliumlike ($1s^22s^2$ singlet) projectiles by s-type wave functions. The total energy of the system calculated here in this way should be compared with any available detailed results. To our regret, however, we do not find good examples, so a comparison was made for a neutral beryllium atom. According to (2.6) and (2.7), the total energy of the neutral Be atom is $E=-386.501$ eV. However, Clementi and Roetti [32] obtained $E_{\text{CR}}=-396.386$ eV, so that the difference $\Delta E=E-E_{\text{CR}}=9.886$ eV. This is due to a rather crude description of the one-electron wave function adopted. Nevertheless, the ratio $\Delta E/E_{\text{CR}}$ amounts to only 2.5%. Moreover, the orbital exponent for the $1s$ state is 3.3716 in our case and 3.47116 in Clementi and Roetti's. Then, we think the trial wave function in the present variational method is not bad. In addition, the ground state is in most cases described by only s-type wave functions [32] as long as a spherically symmetric scalar potential of the nucleus is imposed on the electrons. Judging from these circumstances, the adopted wave functions are reasonable.

Figure 1 shows the calculated stopping power of carbon for O^{q+} ($q=4$–8) ions with velocity from $v=7v_0$ to $v=60v_0$, together with a recent experimental result of Ogawa *et al.* [25] at $v=20.6v_0$ under the frozen-charge-state condition. The mean excitation energy I of carbon is taken to be $I=77.3$ eV$=2.842$ a.u. [1]. The stopping cross section for O^{5+} and O^{4+} ions is calculated on the basis of formula (2.33) while for O^{8+}, O^{7+}, and O^{6+} ions we use formula (1.2). Experimental energy-loss data for a lithiumlike O^{5+} ion were obtained recently [25]. Agreement between the calculated result and the experimental data is quite good, except that the experimental data tend to be slightly larger in every charge state. In general, as the Z_1 value increases, the average radius of the bound electron becomes shorter since, roughly speaking, it is inversely proportional to Z_1. Then the screening of the projectile's nuclear charge by the bound electrons is so complete that the net-charge approximation becomes valid for heavier (or larger-Z_1) ions. The formula (2.33) clearly indicates this fact, showing that the first term plays a dominant role for large Z_1. In other words, the ion can be regarded as a point charge. This picture leads

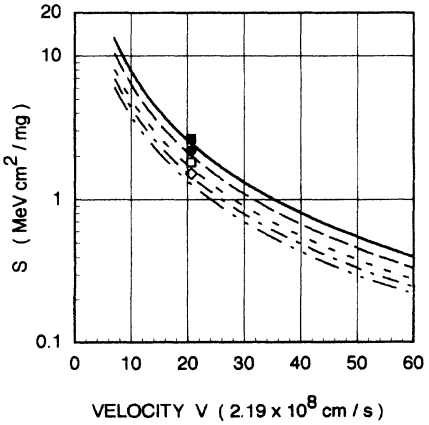

FIG. 1. Stopping power of carbon ($I=77.3$ eV) for O^{q+} ($q=4$–8) ions as a function of velocity. The theoretical results [Eqs. (2.33) and (1.2) are drawn for $q=8$ ——, for $q=7$ — —, for $q=6$ — — —, for $q=5$ —·—·—·, and for $q=4$ —··—··—. The experimental data (Ref. [25]) are plotted for $q=8$: (■), for $q=7$: (●), for $q=6$; (□), and for $q=5$: (◇).

to another conclusion: that the effective stopping-power charge Z_{eff} reduces to the net charge. Thus, the effective charge depends on not only Z_1 but also the ion velocity. We comment that in the comparison between the theoretical and experimental results the higher-order terms (Z_1^3 and Z_1^4 terms) are negligibly small.

Figure 2 shows the effective charge Z_{eff} calculated for O^{q+} ($q=4$–7) ions in collisions with carbon targets at velocities from $v=7v_0$ to $v=60v_0$, and for C^{q+} ($q=4,5$) ions from $v=5v_0$ to $v=60v_0$, together with recent experimental data. From the figure, one can see that the effective charge of a particularly stripped ion increases with velocity in any charge state. At very high velocities, the effective charge is at least saturated, to be the constant given by Eq. (2.37) or (2.39). Agreement of the calculated values with the experimental data is quite good. The figure shows that the effect of bound electrons attached to a projectile is important even at high velocities.

In order to estimate the screening charge in the stopping power per bound electron, we calculate $Z_{\text{SC}}(q,q-1)$ in Eq. (2.41). Figure 3 shows the curves of $Z_{\text{SC}}(q,q-1)$ as a function of velocity v calculated for O^{q+} ($q=4$–8) and C^{q+} ($q=4$–6) ions passing through a carbon target. The values derived from recent experimental data are also plotted. At a glance one can find two remarkable features. First, the six curves drawn can be classified into two groups, namely, four curves with $1s$-state screening and the rest with $2s$-state screening. Second, the velocity dependence of $Z_{\text{SC}}(q,q-1)$ for $1s$-state screening is different from that for $2s$-state screening. At $v=7v_0$ the $1s$ electron can screen the projectile's nuclear charge by $0.9e$. This amount decreases slightly and monotonically with increasing velocity and at last saturates and becomes constant. On the other hand, the screening charge by the $2s$ electron is nearly constant ($0.4e$) over the velocity range considered. At high velocities, in fact, the effective charge can be described by Eqs. (2.37) and (2.39). Except for $Z_{\text{SC}}(5,4)$ for the carbon-ion case, the screening charges [$Z_{\text{SC}}(8.7)$, $Z_{\text{SC}}(7,6)$, and $Z_{\text{SC}}(6,5)$ for the oxygen-ion case and $Z_{\text{SC}}(6,5)$ for the carbon-ion case] derived from experiment support the theoretical results. The discrepancy between theoretical and experimental values in $Z_{\text{SC}}(5,4)$ for the carbon-ion case is due to the fact that, as was shown in Fig. 2, the measured stopping power of carbon (or the effective charge) for 126.4-MeV C^{4+} ions is slightly larger than the theoretical value, in contrast with that for a C^{5+} ion.

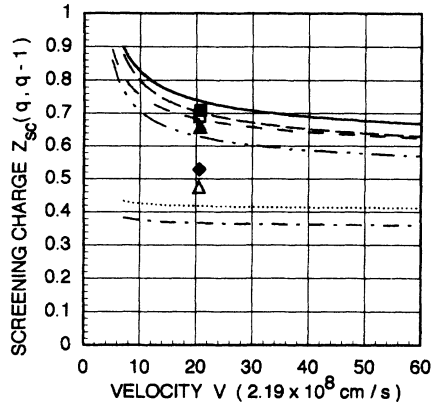

FIG. 3. Screening charge $Z_{\text{SC}}(q,q-1)$ per $1s$ or $2s$ electron on oxygen and carbon ions. Theoretical results are for oxygen ions ($q=8$, ——; $q=7$, — —; $q=6$, · · · ·; and $q=5$ —·—·—·) and for carbon ions ($q=6$, — — —; and $q=5$, —·—·—) and the experimental data are for oxygen ions (from Ref [25]) ■, ($q=8$; ▲, $q=7$; ♦, $q=6$) and for carbon ions (from Ref [23] (□, $q=6$; and △, $q=5$).

In order to have a universal feature, a scaling of the existing stopping power would be useful. In fact, we can scale the stopping-power curves for four types of projectiles with relatively high accuracy by seeking a best-fit value α of the scaling factor Z_1^{α}. First, we plotted the calculated stopping-power values of the H-like projectiles with $Z_1=2$, 3, 4, 5, 6, 10, and 20 at $v=20v_0$, and found a value of $\alpha_{20}=2.180$ which best reproduces the Z_1 dependence of the stopping power. Following the same pro-

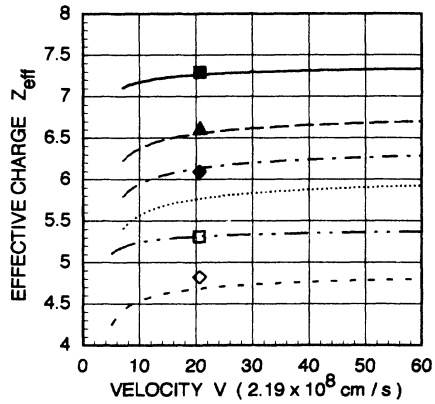

FIG. 2. Effective charge of O^{q+} ($q=4$–7) ions and O^{q+}($q=4,5$) ions passing through carbon foils as a function of velocity, the theoretical results (——, O^{7+}; — —, O^{6+}; —·—·—·, O^{5+}; · · · ·, O^{4+}; —·—·—, C^{5+}; and — — —, C^{4+}) and the experimental data (■, O^{7+}; ▲, O^{6+}; ♦, O^{5+}; □, C^{5+}; and ◇, C^{4+}) obtained from Refs. [23] and [25].

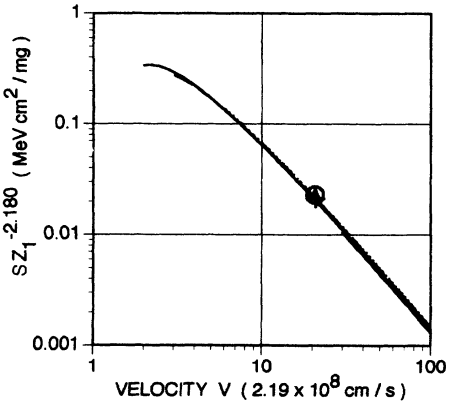

FIG. 4. Scaled stopping cross section $SZ_1^{-2.180}$ vs ion velocity v for hydrogenlike ions penetrating carbon foils. The theoretical curves are drawn for $Z_1=2$, 3, 6, 10, 20, and 30, respectively, in the velocity range $Z_1v_0 \leq v \leq 100v_0$. The experimental data are plotted for O^{7+}, ▲ (Ref. [25]); C^{5+}, ○ (Ref. [23]); and He^+, + (Ref. [22]).

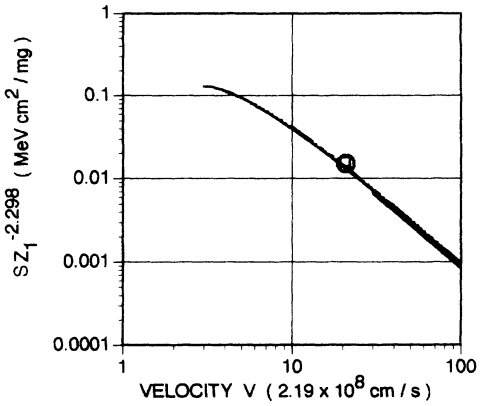

FIG. 5. Scaled stopping cross section $SZ_1^{-2.298}$ vs ion velocity v for heliumlike ions penetrating carbon foils. The theoretical curves are drawn for $Z_1=3$, 4, 6, 10, 20, and 30, respectively, in the velocity range $Z_1v_0 \le v \le 100v_0$. The experimental data are plotted for O^{6+}, ○ (Ref. [25]) and C^{4+}, □ (Ref. [23]).

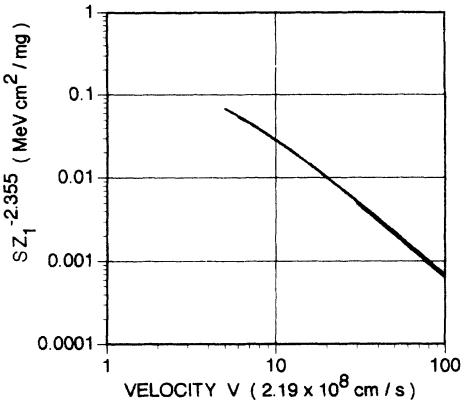

FIG. 7. Scaled stopping cross section $SZ_1^{-2.355}$ vs ion velocity v for berylliumlike ions penetrating carbon foils. The theoretical curves are drawn for $Z_1=5$, 6, 10, 20, and 30, respectively, in the velocity range $Z_1v_0 \le v \le 100v_0$.

cedure, we also found $\alpha_{10}=2.207$ at $v=10v_0$ and $\alpha_{30}=2.160$ at $v=30v_0$. One sees the relative difference $(\alpha_{20}-\alpha_i)/\alpha_{20}=\pm 0.01 (i=10,30)$. For other types of projectiles we obtained the values of α as well. Thus, at high velocities, scaling is available with relatively high accuracy. The relative difference in α is very small, so we use the values of α at $v=20v_0$ as representative for various projectiles. Figures 4–7 display the stopping-power cross-section curves of a carbon target for $Z_1=2$, 3, 4, 5, 6, 10, 20, and 30 and for velocities in the range $Z_1v_0 \le v \le 100v_0$. The ordinate indicates the stopping cross section multiplied by the scaling factors $Z_1^{-2.180}$, $Z_1^{-2.298}$, $Z_1^{-2.330}$, and $Z_1^{-2.355}$ obtained at $v=20v_0$ for the hydrogenlike, heliumlike, lithiumlike, and berylliumlike ions, respectively, while the abscissa denotes the velocity in units of the Bohr velocity v_0 ($=2.19\times10^8$ cm/s). The value of α in the scaling factor becomes slightly larger as the number of bound electrons increases. Here the relativistic effect is not considered. It might seem curious that the value of α in the scaling factor is larger than 2. Since the bound electrons screen the nuclear charge of a projectile, one might expect the Z_1 dependence of the stopping for the present projectiles to be weaker than that for a point charge, which is proportional to Z_1^2 [3]. However, this is not correct. The screening effect works more strongly at low Z_1 than at high Z_1. Consequently, the stopping values for light (low-Z_1) ions are suppressed, while those for heavy (high-Z_1) ions are almost unchanged from the bare values.

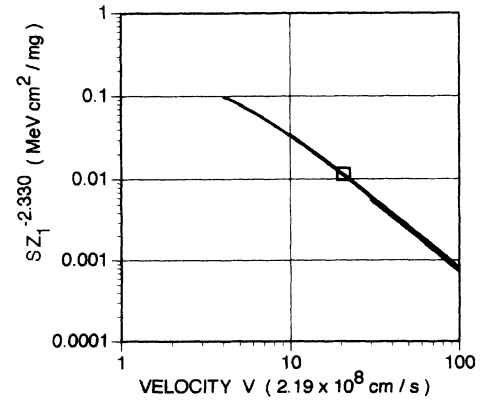

FIG. 6. Scaled stopping cross section $SZ_1^{-2.330}$ vs ion velocity v for lithiumlike ions penetrating carbon foils. The theoretical curves are drawn for $Z_1=4$, 5, 6, 10, 20, and 30, respectively, in the velocity range $Z_1v_0 \le v \le 100v_0$. The experimental data are plotted for O^{5+}, □ (Ref. [25]).

Finally we discuss the contribution of the projectile's excited states. In principle, inclusion of those excited states is possible [28,31]. However, we do not need to take into account these contributions for the following reasons. If a projectile were excited in a foil, electrons in excited states could easily be ionized in the subsequent collisions with much higher probability than those in the ground state. According to the Born approximation, the cross section for the electron loss process is inversely proportional to the binding energy of an ionized electron [33,34]. In a hydrogenic model, the electron-loss cross section $\sigma_{\text{loss},n}$ for an excited state with principal quantum number n is given by n^2 times the cross section $\sigma_{\text{loss},g}$ for the ground state. Hence, $d_{\text{pre},n}$ reduces to $(1/n^2)d_{\text{pre},g}$. Thus the mean free path of the ion in the excited state becomes shorter and its attenuation occurs much more rapidly with respect to the foil thickness. Judging from these considerations, we think the contribution of the excited states of a projectile is negligibly small, especially for light ions. For heavier ions, on the other hand, the excited states will be expected to play a nonnegligible role in the stopping on account of the large binding energy. As a matter of fact, the excited states are related to the projectile x-ray emission. From this viewpoint, we have started an evaluation of the energy loss of excited projectiles, and work on two-electron metastable ($1s2s$) ions has been published [35].

In conclusion, an analytical expression for the electronic stopping power for lithiumlike and berylliumlike projectiles in a frozen charge state has been presented on the

basis of first-order perturbation theory and the Hartree-Fock-Slater method. The leading correction term $\Delta L(Z_1,Z_2,v)$ at high velocity was also derived. The effective stopping-power charge of frozen-charge-state projectiles and the screening charge per either the $1s$ the $2s$ electron were presented. Scaling laws were found in the electronic stopping power of carbon for swift hydrogenlike, heliumlike, lithiumlike, and berylliumlike ions. Good agreement was obtained between the theoretical results and recent experimental data. The scaling relations can be found for other target materials.

ACKNOWLEDGMENTS

The author would sincerely like to thank Dr. H. Ogawa and co-workers for the courtesy of sending their experimental results prior to publication. The author appreciates a grant from the Electric Technology Research Foundation of Chugoku.

[1] H. H. Andersen and J. F. Ziegler, *The Stopping and Ranges of Ions in Matter* (Pergamon, New York, 1977).
[2] J. F. Janni, At. Data Nucl. Data Tables **27**, 147 (1982).
[3] H. A. Bethe, Ann. Phys. (Leipzig) **5**, 325 (1930).
[4] F. Bloch, Ann. Phys. (Leipzig) **16**, 285 (1933).
[5] R. H. Ritchie, Phys. Rev. **114**, 644 (1959).
[6] J. Neufeld and R. H. Ritchie, Phys. Rev. **98**, 1632 (1955).
[7] J. Lindhard and A. Winther, K. Dan. Vidensk. Selsk. Mat. Fys. Medd. **34**, No. 4 (1964).
[8] P. Sigmund, Phys. Rev. A **26**, 2497 (1982).
[9] P. M. Echenique, R. M. Nieminen, J. C. Ashley, and R. H. Ritchie, Phys. Rev. A **33**, 897 (1986).
[10] I. Gertner, M. Meron, and B. Rosner, Phys. Rev. A **18**, 2022 (1978); **21**, 1191 (1980).
[11] T. Kaneko, Phys. Rev. A **30**, 1714 (1984); **33**, 1602 (1986).
[12] Toshiaki Kaneko, Phys. Rev. A **40**, 2188 (1989); Phys. Status Solidi B **156**, 49 (1989).
[13] J. Oddershede and J. R. Sabin, At. Data Nucl. Data Tables **31**, 275 (1984).
[14] Toshiaki Kaneko, At. Data Nucl. Data Tables **53**, 271 (1993).
[15] W. H. Barkas, N. J. Dyer, and H. H. Heckman, Phys. Rev. Lett. **11**, 26 (1963).
[16] M. C. Walske, Phys. Rev. **88**, 1283 (1952); **101**, 940 (1956).
[17] T. L. Ferrell and R. H. Ritchie, Phys. Rev. B **16**, 115 (1977).
[18] W. Brandt and M. Kitagawa, Phys. Rev. B **25**, 5631 (1982).
[19] Toshiaki Kaneko, Phys. Rev. A **41**, 4889 (1990); Nucl. Instrum. Methods B **48**, 83 (1990).
[20] B. S. Yarlagadda, J. E. Robinson, and W. Brandt, Phys. Rev. B **17**, 3437 (1978).
[21] N. E. B. Cowern, P. M. Read, C. J. Sofield, L. B. Bridwell, and M. W. Lucas, Phys. Rev. A **33**, 1682 (1984).
[22] H. Ogawa, I. Katayama, H. Ikegami, Y. Haruyama, A. Aoki, M. Tosaki, F. Fukuzawa, K. Yoshida, I. Sugai, and T. Kaneko, Phys. Rev. B **43**, 11 370 (1991).
[23] H. Ogawa, I. Katayama, I. Sugai, Y. Haruyama, M. Tosaki, A. Aoki, K. Yoshida, and H. Ikegami, Phys. Lett. A **167**, 487 (1992).
[24] Toshiaki Kaneko, Phys. Rev. A **43**, 4780 (1991).
[25] H. Ogawa, I. Katayama, I. Sugai, Y. Haruyama, M. Saito, K. Yoshida, M. Tosaki, and H. Ikegami, Nucl. Instrum. Methods B **82**, 80 (1993).
[26] N. Bohr, K. Dan. Vidensk. Selsk. Mat. Fys. Medd. **18**, No. 8, 1 (1948).
[27] See, for example, L. D. Landau and E. M. Lifshitz, *Quantum Mechanics* (Pergamon, London, 1958).
[28] Y.-K. Kim and K.-t. Cheng, Phys. Rev. A **22**, 61 (1980).
[29] G. H. Gillespie and M. Inokuti, Phys. Rev. A **22**, 2430 (1980).
[30] H. A. Bethe and E. E. Salpeter, *Quantum Mechanics of One- and Two-Electron Atoms* (Plenum, New York, 1977).
[31] O. H. Crawford, Phys. Rev. A **39**, 4432 (1989).
[32] E. Clementi and C. Roetti, At. Data Nucl. Data Tables **14**, 177 (1974).
[33] Toshiaki Kaneko, Phys. Rev. A **34**, 1779 (1986).
[34] D. W. Rule, Phys. Rev. A **16**, 19 (1977).
[35] T. Kaneko and H. Tsuchida, J. Phys. B (to be published).